Pergamon

Tetrahedron 54 (1998) 5151–5170

TETRAHEDRON

SYNTHESIS AND PROPERTIES OF C(10) ISOPROPYL AND ISOPROPYLIDENE ANALOGS OF BILIRUBIN

Ari K. Kar and David A. Lightner*

Chemistry Department, University of Nevada, Reno, NV 89557 USA

Received 2 February 1998; revised 6 March 1998; accepted 9 March 1998

Abstract. Analogs of bilirubin with isopropyl (**1**) and isopropylidene (**2**) groups attached to the central C(10) carbon were synthesized and evaluated by a combination of NMR, UV-vis and circular dichroism spectroscopy and molecular dynamics calculations. These methods and $^1H\{^1H\}$-homonuclear Overhauser effect (NOE) experiments in $CDCl_3$ solutions indicate that the rubins' carboxylic acid groups are tethered to the dipyrrinone lactams and/or pyrroles by intramolecular hydrogen bonds and confirm that the pigments adopt a folded, ridge-tile shape in solution.

INTRODUCTION

Bilirubin (Fig. 1) is the end-product of heme metabolism in mammals. Best known as the colorful herald of hepatobiliary disease,[1,2] bilirubin is also the toxic agent in kernicterus,[1-3] the major component of pigment gallstones,[3] and an endogenous inhibitor of free-radical injury.[4] In the form of its ester conjugates with sugars, it is the principal pigment in bile.[1-3,5] Bilirubin and its analogs have been studied extensively as paradigmatic models for hepatic glucuronidation and for carrier-mediated hepatic uptake and excretion.[5]

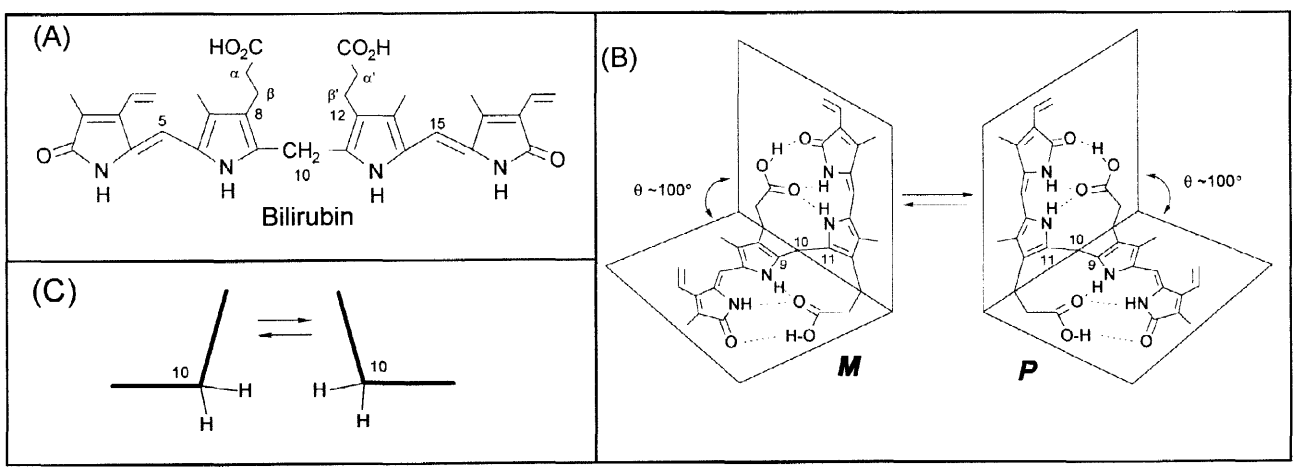

FIGURE 1. (A) Constitutional structure of bilirubin. (B) Conformational representations for ridge-tile-shape ***M*** and ***P*** chirality, intramolecularly hydrogen-bonded, interconverting enantiomers of bilirubin. Hydrogen bonds are shown by dotted lines. (C) Edge view of the bilirubin ridge-tile conformations showing the C(10) hydrogens at the seam.

0040-4020/98/$19.00
PII: S0040-4020(98)00254-3

Bilirubin is conformationally flexible in solution, but one conformation is significantly more stable than all the others: a folded ridge-tile structure with intramolecular hydrogen bonds between the pyrrole and lactam functions of the dipyrrinone halves and the propionic carboxyl (or carboxylate) groups (Fig. 1B).[6-8] Although bilirubin can form porphyrin-like helical conformers, they are of relatively high energy, and the linear conformation (Fig. 1A) is especially high energy.[7,9] The ridge-tile conformation is the only one that has been observed in crystals of bilirubin[6] and its carboxylate salts.[8] Early spectroscopic studies, particularly NMR,[10,11] supported by energy calculations,[12,13] indicate that hydrogen-bonded ridge-tile conformers also prevail in solution,[14] even in the dipolar protophilic solvent dimethyl sulfoxide.[10,15] Individual ridge-tile conformers of bilirubin are chiral. Both enantiomers occur in solution[7,16] and interconvert rapidly (Fig. 1B)[10] via a succession of non-planar intermediates in which the hydrogen bonding network is never completely broken.[7,9] Low energy rotations about the C(9)-C(10) and C(10)-C(11) bonds lead to opening or closing of the interplanar angle from ~60° to ~130°, while maintaining hydrogen bonding (Fig. 1).[7,14a] Larger rotations break hydrogen bonds and lead to energetically disfavored conformations.

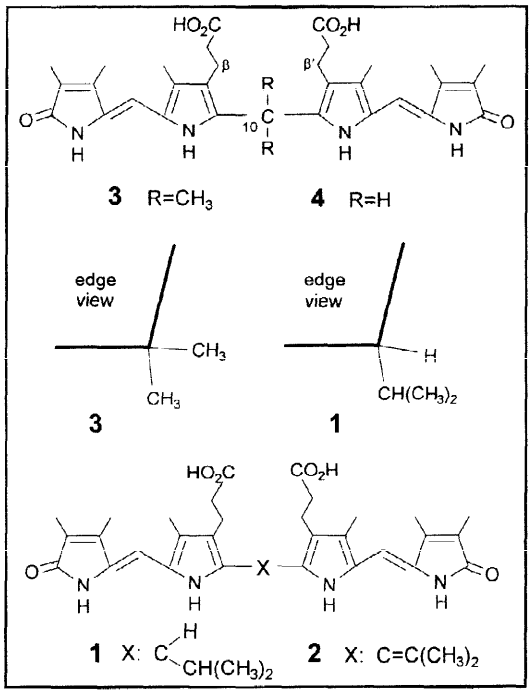

Bilirubin and its analog **4** are insoluble in water and in dilute bicarbonate. Yet, a derivative of **4** with two methyl groups at C(10) on the ridge-tile seam (**3**) was found to increase the pigment's solubility in organic solvents and, seemingly contradictorily, render the pigment soluble in dilute aq. bicarbonate.[17a] The reason for this is unclear because C(10) substituents are far removed from and project away from the hydrogen bonding region. In the ridge-tile conformation, however, the C(10) methyls are sterically compressed against the β,β′ CH_2 groups of the propionic acids, and this internal steric interaction is thought to cause a widening of the ridge-tile interplanar angle.[17b] The purpose of the following study is to detect and explore the influence of C(10) substitution on bilirubin's intramolecular hydrogen bonding and solution properties. For this we synthesized two analogs with only one substituent at C(10): isopropyl rubin (**1**) and its isopropylidene analog (**2**).

RESULTS AND DISCUSSION

Synthesis. Falk *et al.*[18] showed that two equivalents of an α-free dipyrrinone (3-ethyl-2,7,8-trimethyl-(10*H*)-dipyrrin-1-one) may be condensed with isobutyraldehyde in the presence of *p*-toluenesulfonic acid catalyst, and then oxidized with DDQ to afford a linear tetrapyrrole with an isopropylidene group at C(10). The reaction is believed to go first to the rubin, which is oxidized (DDQ) to an unstable verdin that rearranges. Following this procedure, which we modified by using trifluoroacetic acid catalyst and deleting the oxidation step, we found that the simple dipyrrinone (2,3,7,8-tetramethyl-(10*H*)-dipyrrin-1-one, **13**)[19] reacted smoothly with isobutyraldehyde at room temperature in dichloromethane solvent to afford the C(10) isopropyl rubin **5** in 52% isolated yield (Synthetic Scheme). As noted earlier for a related compound,[18] attempted oxidation of **5** to its C(10)-isopropyl verdin using DDQ led instead to the double-bond isomerized isopropylidene rubin isomer **6**. During the course of the oxidation, a transient green-blue color developed, due to verdin formation, but this faded to a yellow rubin color.

SYNTHETIC SCHEME

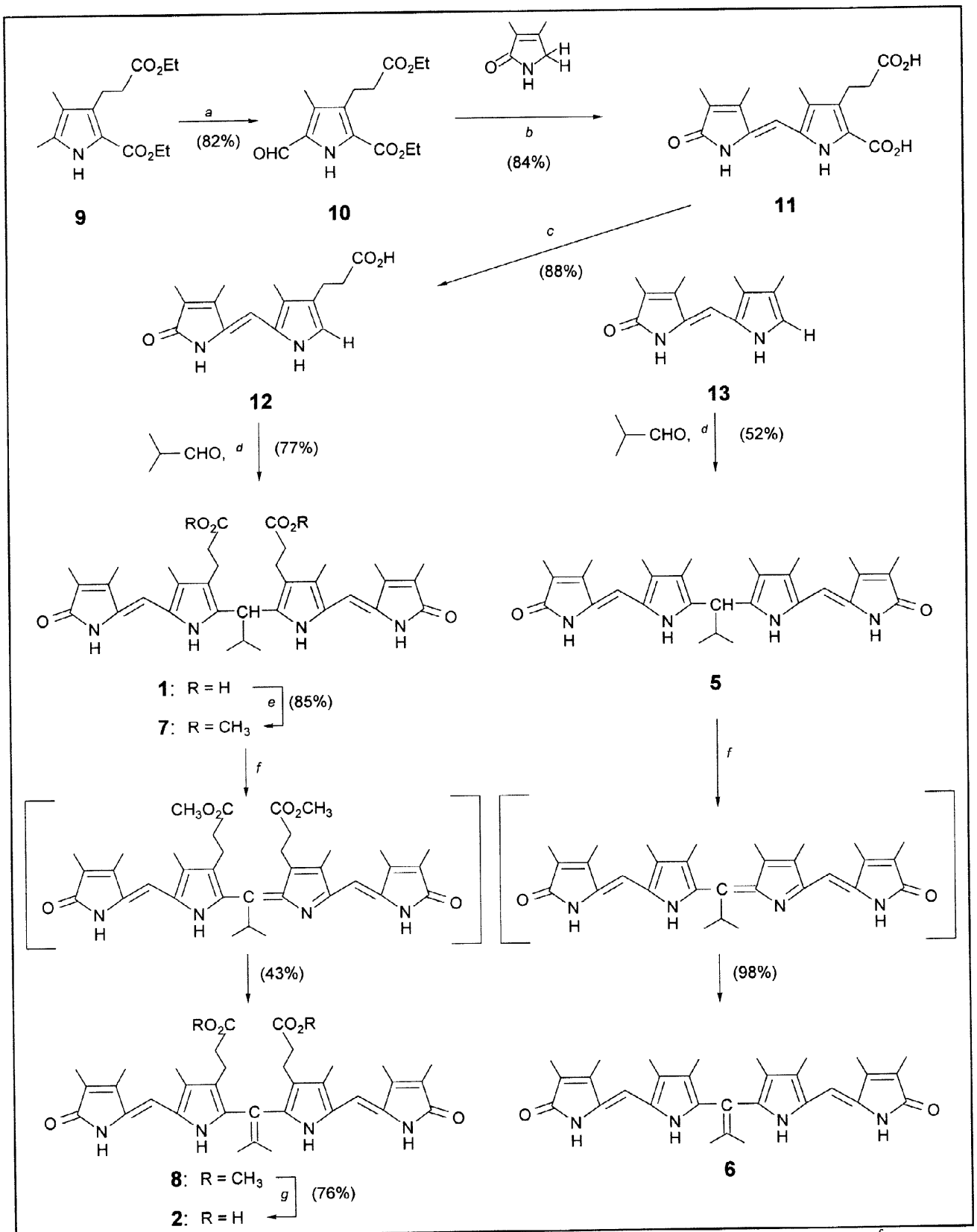

[a] Ceric ammonium nitrate; [b] KOH/CH_3OH; [c] NaOAc-KOAc melt; [d] TFA; [e] $CH_3I/Cs_2CO_3/DMF$; [f] DDQ/THF; [g] $NaOH/CH_3OH$-THF.

Similarly, condensation of dipyrrinone **12** with isobutyraldehyde led to isopropyl rubin **1**. The precursor dipyrrinone (**11**) was prepared by condensation of 3,4-dimethylpyrrolinone[17a] with pyrrole aldehyde **10**. The latter was prepared by ceric ammonium nitrate oxidation[20] of the α-methyl group of ethyl 2,3-dimethyl-(5-ethoxycarbonyl)-1*H*-pyrrole-4-propanoate (**9**)[21] in high yield. As above, attempted oxidation of the rubin dimethyl ester (**7**) with DDQ to its verdin gave only the isopropylidene rubin ester (**8**), which was saponified to give isopropylidene rubin acid **2**. Attempts to isolate the verdin intermediates prior to **6** or **8** were unsuccessful.

Solubility and Chromatographic Properties. Consistent with the attachment of lipid-solubilizing isopropyl and isopropylidene groups, **1** and **2** are 5-10 times more soluble in a nonpolar organic solvent, such as chloroform, than the unsubstituted parent rubin (**4**). Surprisingly, they are also more soluble in polar solvents, such as methanol, and interestingly, while **4** is insoluble in 5% aq. sodium bicarbonate, **1** is soluble but **2** is insoluble. Thus, **1** and **2** are much more amphiphilic than the parent (**4**), and thus mimic the behavior found for **3**.[17] The solubility behavior of **1** and **2** is curious because they have R_f values on silica gel TLC very similar to **3** and **4** (**1**, 0.88; **2**, 0.83; **3**, 0.85; **4**, 0.84) when 3% CH_3OH in CH_2Cl_2 is used as eluent. These values are very similar to that of bilirubin itself (R_f ~0.89). In reverse-phase HPLC, however, distinctly different retention times were noted, for **1** and **2** (22 and 20 minutes, respectively) *vs.* **3** (8.1 min.) and **4** (15 min.). The HPLC data suggest that **1** and **2** are less polar and more lipophilic than their parent (**4**), and seemingly contradictorily, they suggest that **3** is more polar than **4**. Characteristic of rubins whose propionic acid groups are engaged in intramolecular hydrogen bonding, the acids (**1** and **2**) are much more lipophilic than the corresponding dimethyl esters (**7** and **8**) in chromatography: **7**, R_f 0.53 and retention time 6.2 min.; **8**, R_f 0.37 and retention time 4.9 min.

Structure and ^{13}C-NMR Spectra. The ^{13}C-NMR spectra (Table 1) of the isopropyl and isopropylidene rubins are consistent with the constitutional structures shown. Carbon chemical shifts were assigned by analogy with known rubins and by long-range ^{1}H-^{13}C-NMR coupling experiments (HMBC and HMQC) and by homonuclear NOE experiments. The expected chemical shift differences were found at C(10) and C(10^1) and at C(8)/C(12), which are at or close to the new substitution center. Interestingly, the rubin acids (**1, 2, 3, 4**) all exhibit lactam carbonyl chemical shifts that are 1-2 ppm more deshielded than their corresponding dimethyl esters (**7, 8, 15, 16**) or their peralkylated rubin analogs **5** and **6**. Since rubin dimethyl esters and peralkylated rubins are thought to engage in *inter*molecular hydrogen bonding involving dipyrrinone to dipyrrinone hydrogen bonds,[22] the data suggest that acids **1, 2, 3** and **4** do not.

^{1}H-NMR and Hydrogen Bonding. The ^{1}H-NMR data from rubins **1**, **2**, **3**, and **4** (Table 2) are similar in many respects. The backbone methyl groups of the isopropyl (**1**) and isopropylidene (**2**) rubins at C(2)/C(18), C(3)/C(17) and C(7)/C(13) have very similar chemical shifts that are also essentially the same in the parent rubin (**4**) and its *gem*-dimethyl analog (**3**). They shift in consistent, characteristic ways from $CDCl_3$ to $(CD_3)_2SO$ solvent. In the latter, the isopropyl methyls of **1** are equivalent, indicating free rotation and no diastereotopicity. In contrast, in $CDCl_3$ the methyls are no longer equivalent and remain non-equivalent at 60°C, suggesting that the pigment adopts a different or a less mobile conformation in $CDCl_3$. If **1** were to adopt intramolecularly hydrogen-bonded conformations in $CDCl_3$ like those in Fig. 1B, the isopropyl methyls would be diastereotopic.

Evidence for intramolecular hydrogen bonding in **1** and **2** in $CDCl_3$ comes from the characteristic deshielding of the COOH hydrogens and the lactam N(21)/N(24)-Hs due to intramolecular hydrogen bonding between these two functional groups. There is also notable shielding of the pyrrole N(22)/N(23)-Hs due to the magnetic anisotropy afforded by a bent, ridge-tile conformation where these NHs lie above or below the neighboring pyrrole

TABLE 1. ^{13}C-NMR Chemical Shifts[a] and Assignments for Rubin Acids (R=H): **1** (X: CH-iPr), **2** (X: C=C(CH_3)$_2$), **3** (X: C(CH_3)$_2$), **4** (X: CH_2); for Rubin Esters (R=CH_3): **7** (X: CH-iPr), **8** (X: C=C(CH_3)$_2$), **14** (X: C(CH_3)$_2$), **15** (X: CH_2), and for Permethylated Analogs: **5** (Y: CH-iPr), **6** (Y: C=C(CH_3)$_2$).[b]

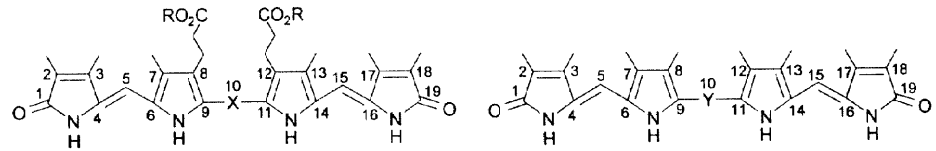

Position[b]	Carbon	Chemical Shift Values[a] in $(CD_3)_2SO$ for Acids				Chemical Shift Values[a] in $(CD_3)_2SO$ for Esters and Permethylated					
		1	**2**	**3**	**4**	**7**	**8**	**14**	**15**	**5**	**6**
1,19	C=O	174.28	174.41	174.05	174.03	173.12	172.41	171.88	172.13	172.39	173.75
2,18	=C-	122.88	122.88	123.19	122.54	122.64	122.69	123.15	123.17	122.82	123/42
2^1,18^1	CH_3	8.68	8.72	8.40	8.10	8.72	8.70	8.49	8.17	8.70	7.96
3,17	=C-	141.81	141.81	141.60	147.23	141.78	141.73	142.12	140.95	141.91	141.76
3^1,17^1	CH_3	9.75	9.57	9.35	9.40	9.59	9.43	9.47	9.59	9.52	9.42
4,16	=C-	130.44	129.79	129.96	130.88	130.05	129.81	130.02	130.33	130.07	129.39
5,15	=CH-	98.48	98.09	98.31	97.80	98.24	97.96	98.41	97.94	98.61	100.50
6,14	=C-	124.58	124.26	124.22	122.00	124.42	124.24	124.58	123.51	124.41	123.95
7,13	=C-	122.21	122.82	121.74	122.90	119.31	122.67	122.11	122.75	122.48	123.71
7^1,13^1	CH_3	9.93	9.94	9.64	9.25	9.93	9.91	9.58	9.25	9.94	9.62
8,12	=C-	119.84	121.38	118.50	119.23	122.58	122.68	118.81	118.97	115.88	116.66
8^1,12^1	CH_2	19.86	20.09	10.81	19.27	19.86	20.07	19.85	19.34	9.94	9.52
8^2,12^2	CH_2/CH_3	35.14	34.29	34.32	34.34	34.43	33.85	34.44	34.12	—	—
8^3,12^3	C=O	172.42	172.42	172.43	172.00	173.07	172.38	173.19	173.31	—	—
8^4,124	OCH_3	—	—	—	—	51.33	51.19	50.95	50.91	—	—
9,11	=C-	133.79	132.56	138.63	128.81	133.87	139.28	138.78	130.57	133.90	133.45
10	C	42.81	123.32	36.59	23.55	43.51	132.51	36.77	23.71	43.42	123.92
10^1	CH_3, CH or C	29.95	121.41	29.07	—	29.30	123.31	29.05	—	29.73	123.35
10^2	CH_3	22.09	22.98	—	—	22.20	22.84	—	—	21.96	21.41

[a] Run at 2.5×10^{-2} M concentration of pigment in $(CD_3)_2SO$ at 22°C. (Values reported in δ (ppm) downfield from $(CH_3)_4Si$. Multiplicities are determined by the APT method.

[b] Superscripts refer to carbons in the β-substituent chains, e.g., 2^1 is the first carbon attached to ring carbon 2.

TABLE 2. ^{1}H-NMR Chemical Shifts, Multiplicities and Assignments for **1** (X: CH-iPr), **2** (X: C=C(CH$_3$)$_2$), **3** (X: C(CH$_3$)$_2$), and **4** (X: CH$_2$) in (CD$_3$)$_2$SO and CDCl$_3$ Solvents.[a]

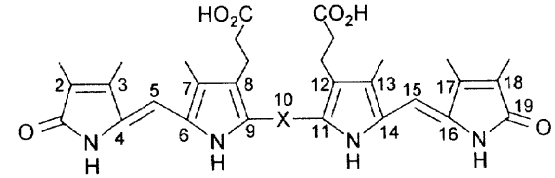

Proton	Chemical Shifts[a] in CDCl$_3$				Chemical Shifts[a] in (CD$_3$)$_2$SO			
	1	**2**	**3**	**4**	**1**	**2**	**3**	**4**
8^3,12^3-CO$_2$H	13.75	13.60 (brs)	13.93 (s)	13.59 (s)	11.93 (brs)	11.81 (brs)	11.90 (brs)	11.89 (brs)
21,24-NH	11.06 (brs), 10.77 (brs)	10.79 (brs)	11.08 (s)	10.61 (s)	9.73 (brs)	10.02 (brs)	9.48 (brs)	9.78 (brs)
22,23-HN	9.17 (brs), 9.13 (brs)	9.16 (brs)	8.91 (brs)	9.15 (s)	9.87 (brs)	10.34 (brs)	10.13 (brs)	10.32 (brs)
5,15-CH=	6.05 (s), 6.01 (s)	6.04 (s)	6.02 (s)	6.04 (s)	5.90 (s)	5.91 (s)	5.95 (s)	5.94 (s)
10-C	4.25 (d)[b]	—	—	4.07 (s)	3.74 (d)[c]	—	—	3.95 (s)
10^1-CH-CH$_3$	2.44-3.32 (m)	—	2.07 (s)	—	2.75 (m)	—	1.73 (s)	—
10^2-CH$_3$	1.19 (d),[d] 0.71 (d)[e]	1.84 (s)	—	—	0.84 (d)[f]	1.81 (s)	—	—
8^1,12^2-α -CH$_A$H$_X$CH$_B$H$_C$CO$_2$H	3.34 (ddd),[ghi] 3.12 (ddd)[hij] 2.71 (ddd),[hik] 2.59 (ddd)[hik]	2.97 (ddd)[hil] 2.54 (ddd)[ikm]	3.50 (ddd)[mno] 2.55 (ddd)[opq]	2.99 (ddd)[ilr] 2.54 (ddd)[ips]	2.79 (t)[t]	2.20 (t)[t]	2.19 (t)[t]	2.41 (t)[t]
8^2,12^2-β -CH$_A$H$_X$CH$_B$H$_C$CO$_2$H	3.03 (ddd),[ghu] 2.96 (ddd)[hjk] 2.85 (ddd),[hku] 2.85 (ddd)[hku]	2.86 (ddd)[lmv] 2.74 (ddd)[hkv]	2.93 (ddd)[mpu] 2.78 (ddd)[mpu]	2.89 (ddd)[kpw] 2.78 (ddd)[rsw]	2.34 (t)[t]	2.18 (t)[t]	1.98 (t)[t]	1.92 (t)[t]
7^1,13^1-CH$_3$	2.15 (s)	2.20 (s)	2.14 (s)	2.16 (s)	2.02 (s)	2.03 (s)	2.06 (s)	2.05 (s)
3^1,17^1-CH$_3$	2.06 (s)	2.05 (s)	2.06 (s)	2.06 (s)	1.94 (s)	1.98 (s)	1.96 (s)	2.00 (s)
2^1,18^1-CH$_3$	1.85 (s)	1.84 (s)	1.85 (s)	1.85 (s)	1.74 (s)	1.75 (s)	1.77 (s)	1.77 (s)

[a] Run at 4 × 10^{-3} M concentration of pigment at 22°C. (Values reported in ppm downfield from (CH$_3$)$_4$Si.) [b] 9.80 Hz; [c] 11.70 Hz; [d] 5.90 Hz; [e] 6.80 Hz; [f] 6.40 Hz; [g] 11.0 Hz; [h] 2.50 Hz; [i] -15.0 Hz; [j] 12.0 Hz; [k] 4.50 Hz; [l] 13.5 Hz; [m] 2.00 Hz; [n] 11.5 Hz; [o] -13.0 Hz; [p] 2.60 Hz; [q] 4.70 Hz; [r] 2.80 Hz; [s] 4.60 Hz; [t] 7.80 Hz; [u] -18.5 Hz; [v] -18.8 Hz; [w] -18.7 Hz.

or dipyrrinone π-electron system.[23] Similar chemical shifts are found in the parent C(10)-unsubstituted rubin (**4**) and its C(10)-*gem*-dimethyl analog (**3**),[17] thus indicating the likelihood that the rubin acids of Table 2 adopt a ridge-tile conformation similar to that of bilirubin (Fig. 1B), where the propionic acid COOH groups and opposing dipyrrinones can engage in intramolecular hydrogen bonding.

Unlike the parent rubin (**4**) and its 10,10-dimethyl (**3**) and 10-isopropylidene (**2**) analogs, 10-isopropyl rubin **1** exhibits two non-identical sets of dipyrrinone NH chemical shifts in $CDCl_3$: 11.06 and 9.17 ppm; 10.77 and 9.13 ppm for the lactam and pyrrole NHs, respectively. These data indicate molecular dissymmetry in the intramolecularly hydrogen bonded ridge-tile conformation.[24] The ridge-tile conformers of **2**, **3** and **4** have C_2-symmetry; in **1** they do not. The nonequivalence of proton signals in **1** suggests slow conformational inversion of the type shown in Fig. 1B and a weakening of intramolecular hydrogen bonds in the half where the isopropyl group exerts a non-bonded steric buttressing effect on one of the propionic acid β-methylene groups.

Further support for the intramolecularly hydrogen-bonded ridge-tile conformation comes from analysis of the vicinal H|H coupling in the propionic acid $-C_\beta H_2C_\alpha H_2CO_2H$ segments of **1**, **2**, **3** and **4**. Confirming a molecular shape where the propionic residues are constrained to adopt fixed molecular conformations, the H|H coupling constants indicate an ABCX pattern consistent with a fixed staggered propionic acid segment geometry (Table 3) — as has been reported previously for bilirubin.[10] The α-hydrogens (H_B and H_C) at C(8^2) and C(12^2) and the β-hydrogens (H_A and H_X) at C(8^1) and C(12^1) show vicinal coupling constants characteristic of torsion angles (H_A-C-C-H_C, H_X-C-C-H_B and H_X-C-C-H_C) of ~60°, while (H_A-C-C-H_B) is ~180°. They are clearly not the typical averaged ^3J values found in the spectra run in $(CD_3)_2SO$ solvent, and found in dipyrrinones in either solvent. In those cases, there is greater conformational flexibility in the propionic segment, whose CH_2 groups appear as triplets (A_2B_2 pattern).

Unlike the more symmetric rubins (**2**, **3** and **4**), isopropyl rubin **1** exhibits two sets of ABCX patterns for the propionic acid α and β CH_2 signals in $CDCl_3$. These data, too, indicate that in its intramolecularly hydrogen-bonded conformation **1** does not exhibit the expected C_2-symmetry of the tetrapyrrole framework. One triad of carboxylic acid to dipyrrinone hydrogen bonds is intrinsically different from the other due to a geometric distortion forced by intramolecular nonbonded steric interactions from the C(10) isopropyl group.

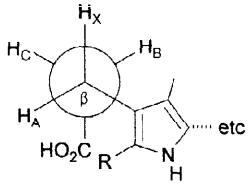

TABLE 3. ^{1}H-NMR Chemical Shifts[a] and Couplings in the $CH_AH_XCH_BH_CCO_2H$ Propionic Acid Fragment of Bilirubin Analogs in $CDCl_3$ Solvent at 22°C.

Pigment	Chemical Shift (δ, ppm)[a]				Coupling Constant (J, Hz)					
	H_A	H_B	H_C	H_X	J_{AB}	J_{AC}	J_{AX}	J_{BC}	J_{BX}	J_{CX}
14: R= CH_2	2.99	2.89	2.78	2.54	13.5	2.8	-15.0	-18.7	2.6	4.6
13: R= $C(CH_3)_2$	3.50	2.98	2.78	2.55	11.5	2.0	-13.0	-18.5	2.6	4.7
2: R= C=$C(CH_3)_2$	2.97	2.86	2.74	2.54	13.5	2.5	-15.0	-18.8	2.0	4.5
1: R= CH(i-Pr)[b]	3.34 3.12	3.03 2.96	2.85 2.85	2.71 2.59	11.0 12.0	2.5 2.5	-15.0 -15.0	-18.5 -18.5	2.5 2.5	4.5 4.5

[a] In ppm downfield from $(CH_3)_4Si$ for 10^{-3} M solutions in $CDCl_3$. [b] Two sets of protons.

Nuclear Overhauser Effect. Additional evidence for intramolecular hydrogen bonding and thus for ridge-tile conformations in **1** and **2** come from $^1H\{^1H\}$-homonuclear NOEs found between the CO_2H proton and the lactam NHs, and between the lactam NHs and pyrrole NHs. The former indicate a close proximity between the acid and lactam groups, as is found when they are linked by hydrogen bonding; the latter indicate a *syn-Z* configuration of the dipyrrinones, which is confirmed by the NOEs seen between the C(5) and C(15)-Hs and the nearby CH_3 groups.[10] Interestingly, while we could detect no NOEs from the isopropylidene methyl groups, the isopropyl methyls exhibited NOEs with the propionic acid β-CH_2 groups.

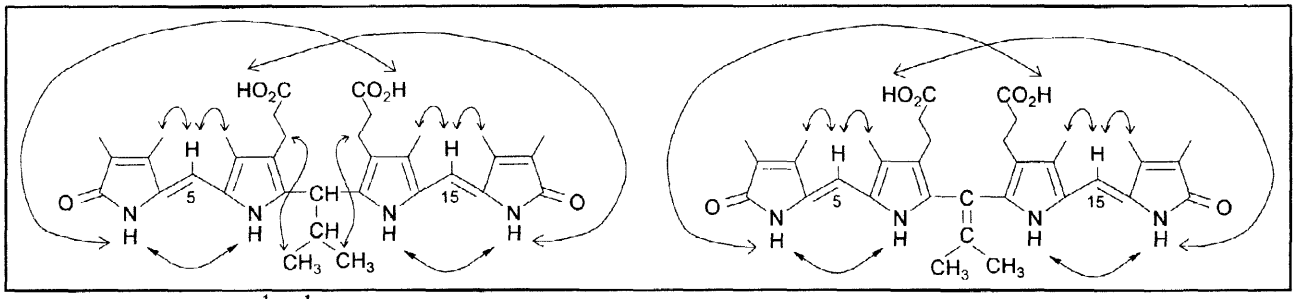

FIGURE 2. Important $^1H\{^1H\}$-homonuclear Overhauser effects shown by double-headed arrows in **1** and **2** in $CDCl_3$.

Conformational Analysis from Molecular Dynamics Calculations. Additional insight into the influence of C(10) isopropyl and isopropylidene substituents on bilirubin conformation may be gained from molecular dynamics calculations.[7] Using the force field in SYBYL,[25] conformational energy maps (Figs. 3 and 4) can be constructed by rotating the dipyrrinone units of **1** and **2** independently about the C(9)-C(10) and C(10)-C(11) bonds, corresponding to torsion angles ϕ_1 and ϕ_2, respectively. With ϕ_1 and ϕ_2 defined as 0° in a porphyrin-like conformation, a large array of conformations can be created through rotations about ϕ_1 and ϕ_2, including the linear conformation (Fig. 2) with $\phi_1 = \phi_2 = 180°$. Figures 3 and 4 show a mapping[7,25] of conformational energy *vs* rotation angles, ϕ_1 and ϕ_2 for **1** and **2**, respectively. Some conformations are greatly stabilized through intramolecular hydrogen bonding,[7,9,13] but even the absence of intramolecular hydrogen bonds, as in **5** and **6**, the global energy minimum conformation is nearly the same as those of **1** and **2** and other bilirubin pigments[26] — a ridge-tile shape.[6-9] As in the parent (**4**)[17b] intramolecular hydrogen bonding stabilizes the ridge-tile conformation of **1** and **2**. The presence of C(10) isopropyl and isopropylidene groups apparently adds further stabilization by raising the energy of local minima. Molecular dynamics calculations find global energy minima corresponding to identical enantiomeric structures for **1** (and for **2**) with each enantiomer being represented by several different wells on the surfaces of Figs. 3 and 4. Thus, isoenergetic global minima are found for identical ***M***-helicity conformers near (ϕ_1 ,ϕ_2) ~ (-60°,-60°), (+300°, -60°), (-60°,+300°) and (+300°,+300°) and for the isoenergetic ***P***-helicity conformer located near (ϕ_1,ϕ_2) ~ (+60°,+60°). Intramolecular hydrogen bonding forces the molecule to adopt a basic three-dimensional molecular structure where the two dipyrrinone chromophores lie in nearly orthogonal planes with dihedral angles of 94° in **1** and 88° in **2**.

The ***M*** and ***P*** conformational enantiomers of **1** and **2** (Figs. 3 and 4) interconvert over barriers calculated to be significantly higher (27-32 kcal/mole) than those of the parent rubin (**4**) (19-22 kcal/mole) and its C(10) *gem*-dimethyl analog (**3**) (15-17 kcal/mole).[17] The interconversion occurs by breaking 3-4 hydrogen bonds while the dipyrrinones are rotated about ϕ_1 and ϕ_2, then remaking the hydrogen bonds.[7] From an examination of Fig. 3, two distinct low energy interconversion pathways are found in **1** to take the ***P***-helicity conformer to the ***M***: (i) A route from (ϕ_1=ϕ_2 ~60°) → (ϕ_1 ~10°, ϕ_2 ~90°) → (ϕ_1~ -40°, ϕ_2 ~90°) → (ϕ_1~ -40°, ϕ_2 ~120°) → (ϕ_1~ -40°, ϕ_1~180°) → (ϕ_1~ -60°, ϕ_2 ~180°) and down to (ϕ_1~ -60°, ϕ_2 ~300°) with an activation barrier of ~28 kcal/mole.

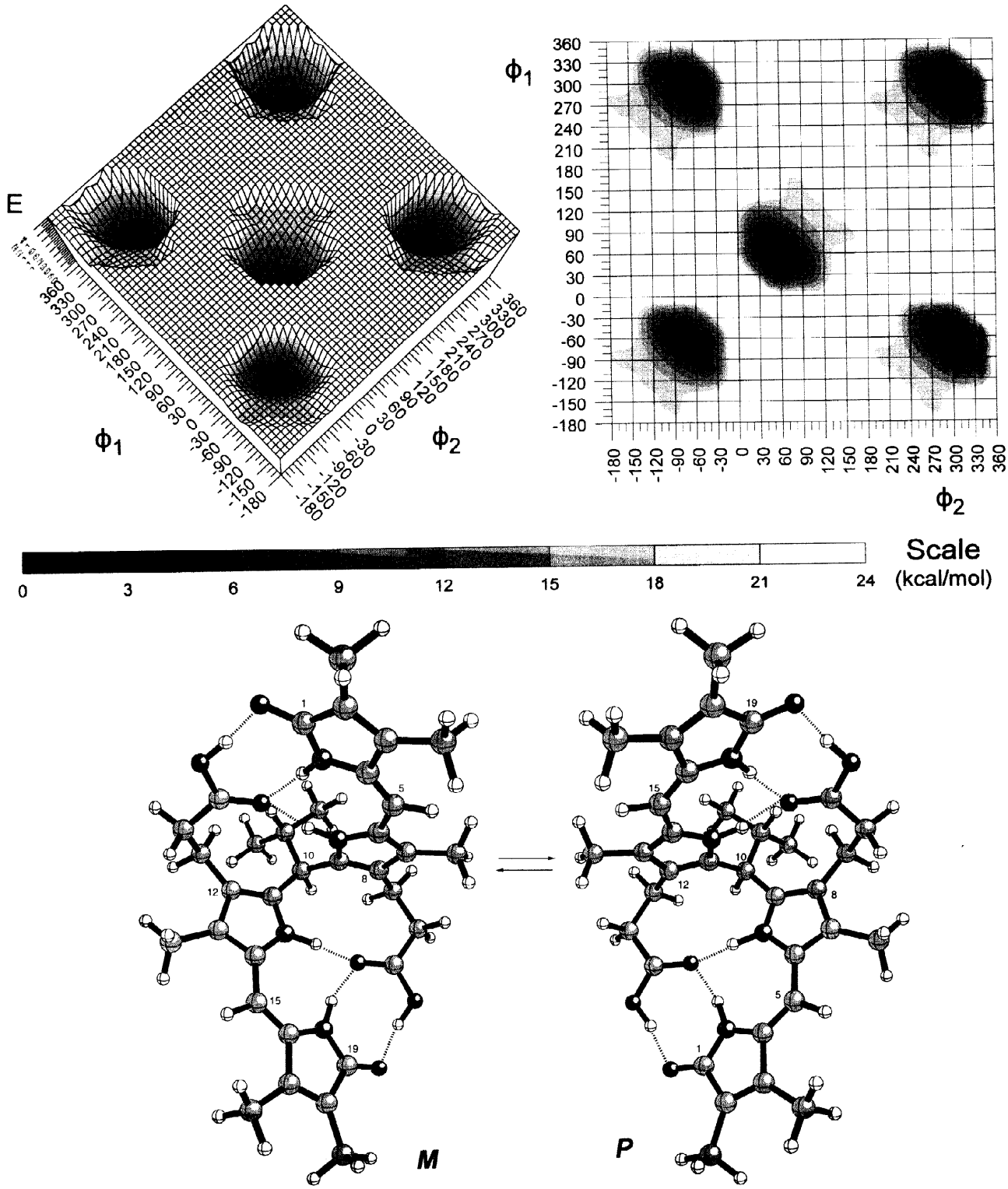

FIGURE 3. (Upper Left) Potential energy surface and (Upper Right) contour map for 10-isopropylrubin (**1**) conformations generated by rotating the two dipyrrinone groups independently about the C(9)-C(10) and C(10)-C(11) bonds (ϕ_1 and ϕ_2 respectively). The energy scale (Middle) is in kcal/mol, and global minima (set to 0 kcal/mol) are found near (ϕ_1, ϕ_2) ~ (-60°, -60°), (-60°, +300°), (+300°, -60°), (+300°, +300°) (***M***-chirality) and near (ϕ_1, ϕ_2) ~ (+60°, +60°) (***P***-chirality). (Lower) Ball and stick conformational representations for the ridge-tile shape ***M*** and ***P*** intramolecularly hydrogen bonded enantiomers. of **1**.

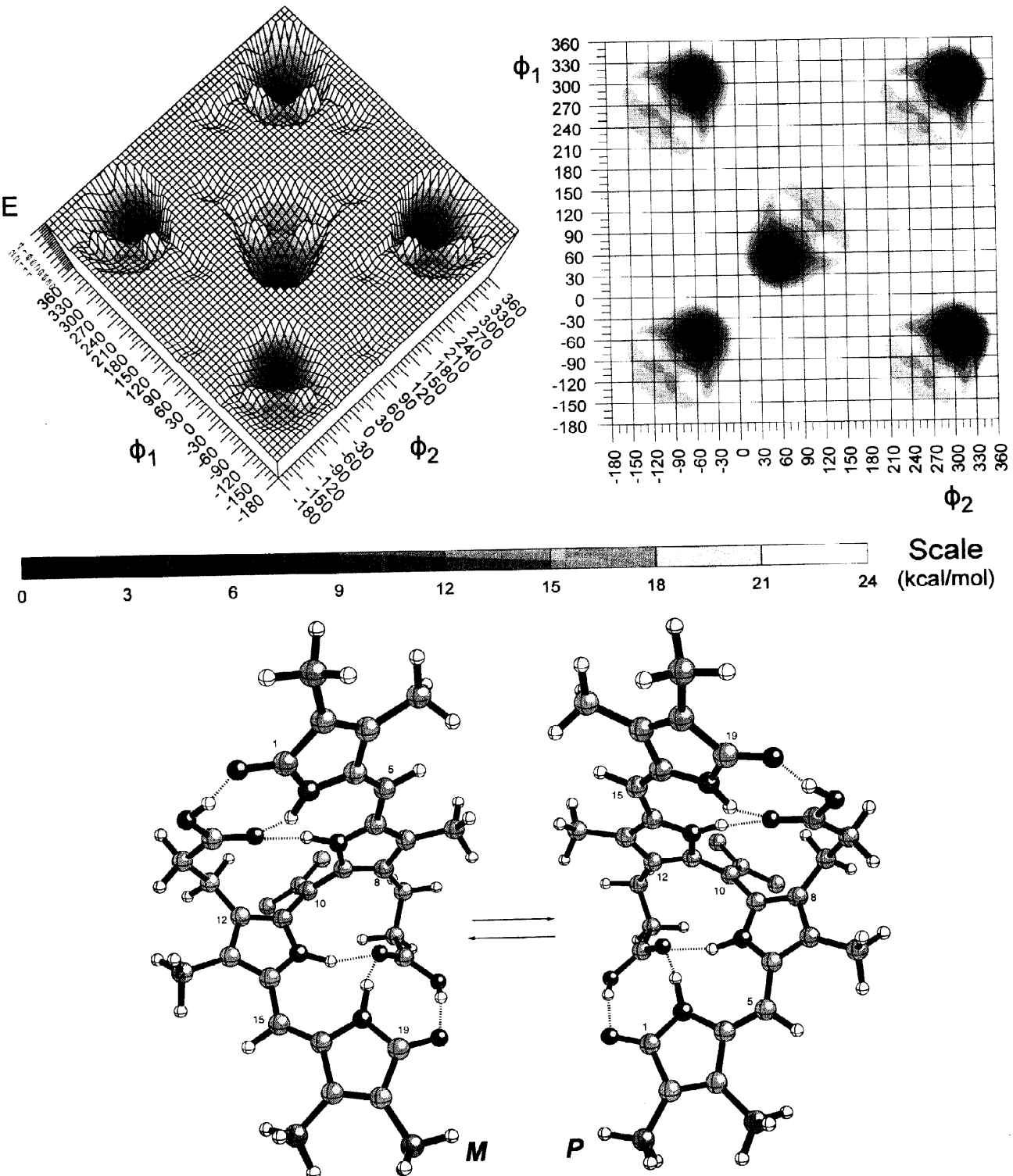

FIGURE 4. (Upper Left) Potential energy surface and (Upper Right) contour map for isopropylidenerubin (**2**) conformations generated by rotating the two dipyrrinone groups independently about the C(9)-C(10) and C(10)-C(11) bonds (ϕ_1 and ϕ_2 respectively). The energy scale (Middle) is in kcal/mol, and ***M***- chirality global minima (set to 0 kcal/mol) are found near (ϕ_1, ϕ_2) ~ (−50°, −50°), (−50°, +310°), (+310°, −50°), and (ϕ_1, ϕ_2) ~ (+310°, +310°). An isoenergetic ***P***-chirality global minimum is found near (ϕ_1,ϕ_2) ~ (+50°, +50°). (Lower) Ball and stick conformational representations for the ridge-tile shape ***M*** and ***P*** intramolecularly hydrogen bonded enantiomers of **2**. The hydrogens of the isopropylidene methyls are removed for clarity of representation.

(ii) A route from (ϕ_1=ϕ_2 ~60°) → (ϕ_1 ~10°, ϕ_2 ~90°) → (ϕ_1~ -40°, ϕ_2 ~90°) → (ϕ_1 ~-80°, ϕ_2 ~60°) → (ϕ_1~ -90°, ϕ_2 ~30°) → (ϕ_1~ -90°, ϕ_1 ~0°), (ϕ_1~ -90°, ϕ_2 ~ -60°) and down to (ϕ_1~ -60°, ϕ_2 ~ -60°), with a barrier of ~32 kcal/mole. In Fig. 4, the two lowest energy pathways for interconverting ***P*** and ***M*** conformational enantiomers of the C(10) isopropylidene rubin **2** are essentially isoenergetic: (i) A route from (ϕ_1 = ϕ_2 ~50°) → (ϕ_1~ -20°, ϕ_2 ~50°) → (ϕ_1~ -50°, ϕ_2 ~60°) → (ϕ_1~ -50°, ϕ_2 +90°) → (ϕ_1~ -50°, ϕ_2 ~150°) → (ϕ_1 ~ -50°, ϕ_2 ~240°) and down to (ϕ_1~ -50°, ϕ_2 ~310°) over a barrier of 27 kcal/mole. (ii) A route from (ϕ_1 = ϕ_2 ~50°) → (ϕ_1 ~ -20°, ϕ_2 ~50°) → (ϕ_1~ -50°, ϕ_2 ~60°) → (ϕ_1~ -50°, ϕ_2 ~30°) → (ϕ_1~ -50°, ϕ_2 ~0°) → (ϕ_1~ -50°, ϕ_2 ~ -20°) and down to (ϕ_1 = ϕ_2 ~ -50°) over a barrier of 28 kcal/mole. The isopropyl group of **1** and isopropylidene group (or C(10) sp^2 carbon) of **2** thus appears to raise the interconversion barrier between the ***M*** and ***P*** ridge-tiles. Such high interconversion barriers suggest the possibility of resolution of **1** and **2** into enantiomers that are stable at room temperature.

Induced Circular Dichroism. As may be seen in Fig. 5, solutions of **1** and **2** in $CHCl_3$ solutions containing a 300:1 molar ratio of quinine:pigment[27] give well-defined, strong bisignate circular dichroism (CD) spectra for the long wavelength UV-visible transition. The CDs are identical in sign but differ in magnitude and spectral center relative to that observed for the parent rubin (**4**) and bilirubin, which are known to exist as a 1:1 mixture of enantiomeric ridge-tile conformers of ***M*** and ***P*** helicity (Fig. 1).[7] In solutions with quinine (Q) the equilibrium Q·***M*** ⇆ Q·***P*** is no longer evenly balanced, and there is an excess of one enantiomeric pigment conformation, with a net CD resulting at the pigment's long wavelength transition. The isopropylidene rubin (**2**) exhibits a CD curve of very nearly the same shape and magnitude as the parent (**4**). The isopropyl rubin (**1**) exhibits a weaker CD, and the reason for the difference is not entirely clear but probably comes from structural distortion due to nonbonded steric repulsions between the C(10)-isopropyl group and one of the propionic acid β-methylene groups.

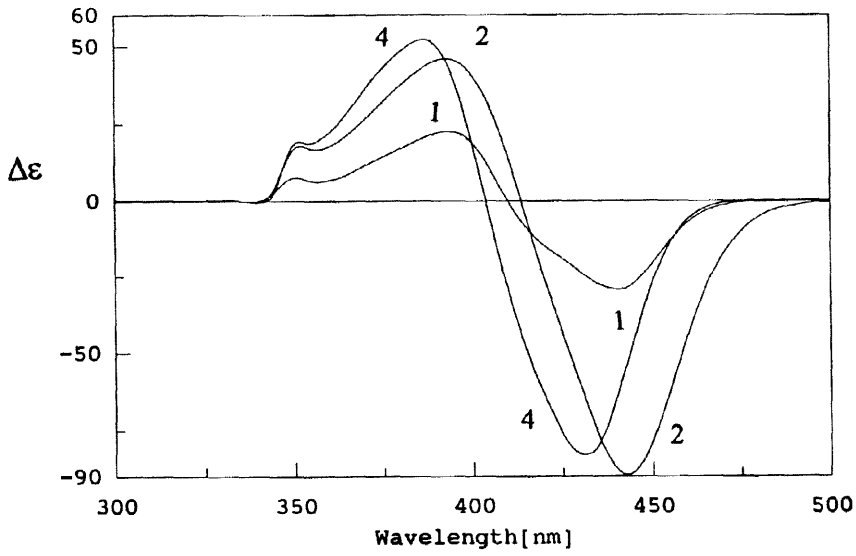

FIGURE 5. Comparison of circular dichroism (CD) spectra of C(10) isopropyl rubin **1**, C(10) isopropylidene rubin **2** and the parent rubin **4** in $CHCl_3$ solvent in the presence of quinine at 22°C. The molar ratio pigment : quinine is 1 : 300, and the concentration of **1**, **2** and **4** are 2.5×10^{-5} M, 3.0×10^{-5} M and 3.0×10^{-5} M, respectively.

Human serum albumin (HSA) is also known to act as a chiral complexation agent for bilirubin and rubin **4**. When bound to HSA and other species' serum albumin, these pigments are known to exhibit optical activity, seen typically as an induced circular dichroism (CD), which is usually intense and bisignate (Fig. 6 and Table 4). In contrast, only very weak induced CDs are found with analogs having no acid groups, *e.g.*, rubin **5**.[20] The protein apparently acts as an enantioselective binding agent for bilirubins with carboxylic acid groups and constrains

the pigment to adopt a chiral conformation. And it is in such a chiral conformation, whether selected by HSA or quinine, that the induced CD occurs through intramolecular exciton coupling[7] between the dipyrrinone chromophores of the rubins. However, unlike bilirubin, its analogs and the C(10) isopropylidene rubin **2**, a reversed bisignate CD is found for C(10) isopropyl rubin **1** in the presence of HSA. The isopropyl group apparently has considerable influence on the enantioselection; whereas, an isopropylidene group does not. Pigment **1** is thus forced to adopt a unique chiral conformation where its component dipyrrinone electric dipole transition moments have a negative exciton chirality.

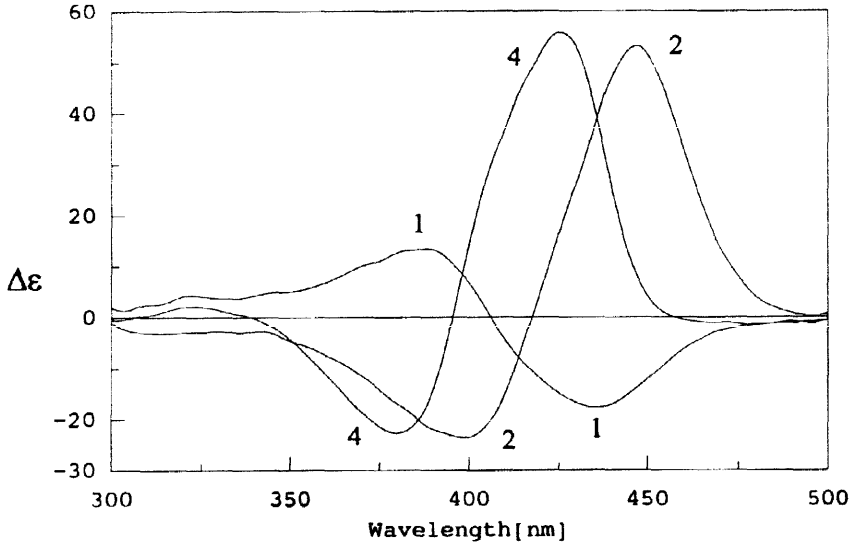

FIGURE 6. Comparison of circular dichroism (CD) spectra of C(10) isopropyl rubin **1** (curve 1), and C(10) isopropylidene rubin **2** (curve 2) on human serum albumin (HSA) with the parent rubin (**4**) on HSA (curve 4) in pH 7.4 Tris buffer at 22°C. The concentration of pigment in each spectrum is 3×10^{-5} M and that of HSA is 6×10^{-5} M, for a 1:2 molar ratio of pigment to albumin.

TABLE 4. Comparison of Circular Dichroism and UV-visible Spectral Data[a] for 10-Isopropyl Rubin (**1**), 10-Isopropylidene Rubin (**2**), Parent Rubin **4** and Bilirubin in pH 7.4 Tris Buffered Aqueous Human Serum Albumin Solutions Containing 2% Dimethylsulfoxide.[b]

	Circular Dichroism			UV-Visible
Pigment	$\Delta\epsilon_{max}$ (λ_1)	λ at $\Delta\epsilon$=0	$\Delta\epsilon_{max}$ (λ_2)	ϵ_{max} (λ)
10-Isopropyl rubin (**1**)	+13 (387)	407	-18 (436)	35,000 (416)^{sh} 39,700 (438)
10-Isopropylidene rubin (**2**)	-24 (398)	416	+53 (447)	51,800 (441)
Parent rubin (**4**)	-24 (384)	407	+56 (429)[d]	36,900 (412)^{sh} 38,500 (430)
Bilirubin	-24 (400)	425	+50 (449)	44,000 (452)

[a] $\Delta\epsilon$ and ϵ in $L \cdot mole^{-1} \cdot cm^{-1}$ and λ in nm; [b] For 2-3 $\times 10^{-5}$ *M* pigment solutions run with 2 mole equivalents of human serum albumin, 30% $(CH_3)_2SO$ has no effect on the BR-HSA CD spectrum.

UV-Visible and Circular Dichroism Spectroscopic Data. The UV-vis data (Table 5) of rubin acids **1**, **2**, **3** and **4** are rather similar, with the long wavelength absorption centered near 425 nm in a range of solvents of varying polarity and hydrogen bonding ability. These data are thus rather like those recorded previously[7] for rubins that engage in intramolecular hydrogen bonding. In contrast, their dimethyl esters (**6**, **7**, **14**, **15**) and analogs with pro-

pionic acids replaced by methyls (**5** and **6**) exhibit λ_{max} shifted to shorter wavelengths (~380-400 nm) in nonpolar solvents due to intermolecular hydrogen bonding.

TABLE 5. UV-Visible Spectroscopic Data[a] for Rubin Acids (R=H): **1** (X: CH-iPr), **2** (X: $C{=}C(CH_3)_2$). **3** (X: $C(CH_3)_2$), **4** (X: CH_2); For Rubin Esters (R=CH_3): **7** (X: CH-iPr), **8** (X: $C{=}C(CH_3)_2$), **14** (X: $C(CH_3)_2$), **15** (X: CH_2); and Permethyl Rubins: **5** (Y: CH-iPr) and **6** (Y: $C{=}C(CH_3)_2$).

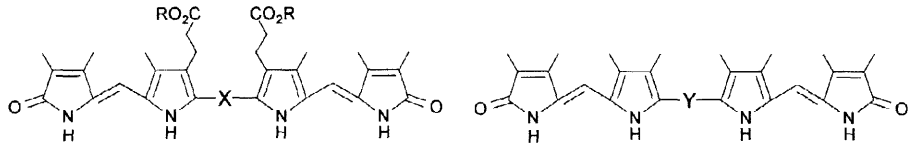

Pigment	ϵ^{max} (λ^{max}) Values in the Specified Solvent					
	C_6H_6	CH_2Cl_2	$CHCl_3$	$(CH_3)_2CO$	CH_3OH	$(CH_3)_2SO$
1	51200 (436)	47500 (420)^{sh} 50600 (437)	49900 (433)	47600 (421)	37700 (402)^{sh} 46500 (430)	38400 (402)^{sh} 49700 (434)
2	45200 (427)^{sh} 46400 (440)	47200 (437)	47400 (439)	47100 (431)	48300 (431)	51800 (437)
3	50600 (434)	50100 (425)	50400 (434)	46300 (426)	46000 (426)	44200 (395)^{sh} 58000 (425)
4	Insol.	51000 (427)	58000 (431)	Insol.	Insol.	57300 (426)
7	59300 (379) 17600 (424)^{sh}	63900 (376)	56300 (380) 49200 (398)^{sh}	61400 (380) 24100 (415)^{sh}	41500 (400) 53400 (432)	40700 (398) 55600 (433)
8	38700 (394) 25200 (416)^{sh}	38700 (399) 36500 (415)^{sh}	43300 (407) 39200 (420)^{sh}	28900 (402)^{sh} 29400 (415)	43600 (440)	45500 (434)^{sh} 48000 (444)
14	36000 (404)	40500 (414)	40700 (414)	40900 (413)	46400 (424)	45500 (420)
15	52700 (384)	57600 (379)	48400 (381) 36600 (411)^{sh}	47000 (381) 34000 (427)^{sh}	47400 (427)	32500 (389)^{sh} 43500 (428)
5	65000 (388) 18600 (425)^{sh}	50300 (382) 44100 (400)^{sh}	48100 (384) 43100 (400)^{sh}	65600 (382) 21300 (417)^{sh}	44500 (381) 25800 (428)^{sh}	40800 (391)^{sh} 43200 (434)
6	61700 (393) 14800 (440)^{sh}	48300 (395)^{sh} 54600 (408)	45600 (400)^{sh} 51600 (408)	58200 (386) 19400 (432)^{sh}	39400 (415)^{sh} 42800 (438)	35700 (441)

[a] λ^{max} in nm, ϵ^{max} in $L \cdot mol^{-1} \cdot cm^{-1}$ for 10^{-5} M solutions.

These data are important because bilirubins are bichromophoric molecules, and the relative orientation of the two dipyrrinone chromophores determines the shape and λ^{max} of the pigment's long wavelength absorption band. UV-visible and circular dichroism spectra are characteristic of two coupled chromophores with little orbital overlap between them and strongly allowed long wavelength transitions. In the case of the ridge-tile conformation of bilirubin (ϵ_{420} ~35,000) (Fig. 1B) maximum exciton interaction between the component dipyrrinone intense long wavelength electronic transitions obtains for a folded conformation, where minimum interchromophoric orbital interaction (homoconjugation) results.[7] However, as the relative orientation of the dipyrrinone chromophores shifts toward the linear conformations (as θ of Fig. 1B increases) or the porphyrin-like (*e.g.*, as θ of Fig.

1B decreases), the spectrum shifts. The porphyrin-like, the ridge-tile and the linear conformations of bilirubins correspond to the classical cases for parallel, oblique and linear orientations of the induced electric dipole transition moments studied in detail by Kasha *et al.*[28] In the ridge-tile conformation (Figs. 1B, 3 and 4), both exciton transitions are allowed and may be seen, *e.g.*, in the pigment's long wavelength UV-visible spectrum as a broad band centered near 430 nm in **4** or as λ^{max} and nearly λ^{sh} (Table 5). As the pigment unfolds toward the linear shape ($\theta \rightarrow 180°$), the UV-visible band is expected to sharpen and red-shift as the transition probability to the lower energy exciton state increases. As the pigment folds more toward a porphyrin shape ($\theta \rightarrow 0°$), the long wavelength UV-visible band is expected to sharpen and blue-shift as the transition probability to the higher energy exciton state increases.

In the C(10)-isopropyl rubin **1**, and C(10)-isopropylidene **2**, the UV-visible spectra exhibit very little solvent dependence, observations consistent with very small conformational changes over the range of solvents studied. This is unlike their esters (**7** and **8**) which showed blue-shifted spectra in non-polar solvents and red-shifted spectra in polar solvents. A similar behavior is found in the parent ester (**15**) and the permethylated analogs (**5** and **6**) of **1** and **2**. Here the data suggest a conformational change from a more folded helical conformation with smaller θ in non-polar solvents to a more open shape in polar solvents. Taken collectively, the UV-visible data implicate the role of much stronger intramolecular hydrogen bonding in **1** than in **2** in nonpolar solvents and relatively unchanged conformations in more polar solvents.

^{1}H-NMR of Dimethyl Esters. Unlike the ^{1}H-NMR spectra of the rubin acids, their dimethyl esters (**7**, **8**, and **15**) in $CDCl_3$ exhibit ordinary triplets for the propionate methylene groups ($-CH_2CH_2CO_2CH_3$) — indicative of unrestricted motion on the NMR timescale. These pigments, as well as those with methyl groups replacing the propionic ester groups (**5** and **6**) also exhibit pyrrole and lactam NH chemical shifts which are very different from those seen in rubin acids (**1-4** of Table 2) in $CDCl_3$ and correspond to the NH chemical shifts (Table 6) typically seen from intermolecular hydrogen bonding. In $(CD_3)_2SO$, however, the NH chemical shifts are more like those of acids **1-4** (Table 2), consistent with the UV-vis data that suggest similar conformations in dimethyl sulfoxide.

TABLE 6. ^{1}H-NMR Chemical Shifts and Assignments of Dimethyl Esters **7** (X: CH-iPr), **8** (X: C=C(CH_3)), **14** (X: C(CH_3)$_2$), **15** (X: CH_2) and Permethylated Rubin **5** (Y: CH-iPr) and **6** (Y: C(CH_3)$_2$ in $(CD_3)_2SO$ and $CDCl_3$ Solvents.[a]

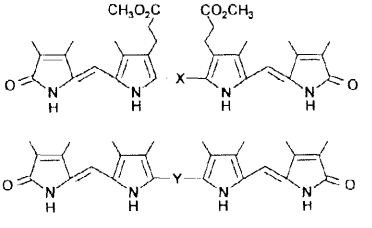

Proton	Chemical Shifts in $(CD_3)_2SO$					Chemical Shifts in $CDCl_3$				
	7	**8**	**5**	**6**	**15**	**7**	**8**	**5**	**6**	**15**
21,24-NH	9.83	9.99	9.67	9.98	9.78	9.92	9.95	11.00	10.35	10.44
22,23-NH	9.93	10.37	9.77	10.02	10.41	9.92	9.95	9.98	10.33	10.28

[a] Run at 4×10^{-3} concentration of pigment at 22°C. Chemical shifts in ppm downfield from $(CH_3)_4Si$.

CONCLUDING COMMENTS

Intramolecular hydrogen bonding between propionic acid CO_2H and dipyrrinone groups is known to be a dominant, conformation stabilizing force in bilirubin and its analogs.[6] The experimental evidence for intramolecular hydrogen bonding in isopropyl rubin **1** is supported by molecular dynamics calculations,[7,25] which indicate a global minimum conformation folded into either a ***P*** or an ***M*** molecular chirality ridge-tile shape that is held in place with six intramolecular hydrogen bonds. The ***M***-helical minima may be found on the conformational energy map at (ϕ_1=ϕ_2~ −60°), (ϕ_1~ +300°, ϕ_2~ −60°), (ϕ_1~ −60°, ϕ_2~ +300°), and (ϕ_1=ϕ_2~ +300°), as shown in Fig. 3. The enantiomeric ***P*** molecular chirality ridge-tile conformation lies at ϕ_1=ϕ_2~ +60° and the lowest energy interconversion pathway between ***M*** and ***P*** chirality conformers lies some 28 kcal/mole above the global minima. The experimental evidence for intramolecular hydrogen bonding in isopropylidene rubin **2**, also supported by molecular dynamics calculations, shows global energy minima (Fig. 4) near (ϕ_1=ϕ_2~ −50°), (ϕ_1~ −50°, ϕ_2~ +310°), (ϕ_1~ +310°, ϕ_2~ −50°) and (ϕ_1=ϕ_2~ +310°), corresponding to the ***M*** molecular chirality conformer of Fig. 4. The global minimum corresponding to the ***P*** molecular chirality conformer is found near (ϕ_1=ϕ_2 ~ +60°), and the ***M*** ⇆ ***P*** interconversion barrier is computed at ~27 kcal/mole.

The current study shows that even when an isopropyl or isopropylidene group is located at C(10), intramolecular hydrogen bonding persists in non-polar solvents. Such rubins are much more amphiphilic than the parent rubin while being constrained to adopt a ridge-tile shape. The C(10) isopropyl group introduces a molecular dissymmetry with one half of the molecule accommodating less effective intramolecular hydrogen bonding.

EXPERIMENTAL

General Procedures. All ultraviolet-visible spectra were recorded on a Perkin-Elmer λ-12 spectrophotometer, and all circular dichroism (CD) spectra were recorded on a Jasco J-600 instrument. Nuclear magnetic resonance (NMR) spectra were obtained on GE QE-300 or GE GN-300 spectrometers operating at 300-MHz, or on a Varian Unity Plus 500-MHz spectrometer in $CDCl_3$ solvent (unless otherwise specified). Chemical shifts were reported in δ ppm referenced to the residual $CHCl_3$ ^1H signal at 7.26 ppm and ^{13}C signal at 77.0 ppm. A J-modulated spin-echo experiment (*A*ttached *P*roton *T*est) was used to assign ^{13}C-NMR spectra. Melting points were taken on a Mel-Temp capillary apparatus and are uncorrected. Combustion analyses were carried out by Desert Analytics, Tucson, AZ. Analytical thin layer chromatography was carried out on J.T. Baker silica gel IB-F plates (125 μ layers). Flash column chromatography was carried out using Woelm silica gel F, thin layer chromatography grade. Radial chromatography was carried out on Merck Silica Gel PF_{254} with gypsum preparative layer grade, using a Chromatotron (Harrison Research, Inc., Palo Alto, CA). HPLC analyses were carried out on a Perkin-Elmer Series 4 high performance liquid chromatograph with an LC-95 UV-visible spectrophotometric detector (set at 410 nm) equipped with a Beckman-Altex ultrasphere-IP 5 μm C-18 ODS column (25 × 0.46 cm) and a Beckman ODS precolumn (4.5 × 0.46 cm). The flow rate was 1.0 mL/minute, and the elution solvent was 0.1 M di-*n*-octylamine acetate in 5% aqueous methanol pH 7.7, 31 °C). Spectral data were obtained in spectral grade solvents (Aldrich or Fisher). Trifluoroacetic acid, isobutyraldehyde, DDQ, and cesium carbonate were from Aldrich. Dichloromethane, methanol, acetic acid, ceric ammonium nitrate, phosphorus pentoxide, N,N-dimethylformamide and tetrahydrofuran were from Fisher. Iodomethane was purchased from Acros.

Ethyl 2-formyl-3-methyl-(5-ethoxycarbonyl)-1*H*-pyrrole-4-propanoate (10). Ethyl 2,3-(5-ethoxycarbonyl)-dimethyl-1*H*-pyrrole-4-propanoate (**9**)[21] (10.0 g, 37.5 mmol) was placed in a 2-L 3-neck round bottom flask equipped with a mechanical stirrer, and 300 mL of THF, 600 mL of glacial acetic acid, and 500 mL of water were added with stirring. The mixture was cooled to 0°C, and 83.0 g (0.154 moles) of ceric ammonium nitrate (CAN) was added. The ice bath was removed and the reaction was allowed to stir for one hour. The mixture was then transferred to a 4 L separatory funnel and 800 mL of water was added. The aqueous solution was extracted with CH_2Cl_2 (3 × 100mL). The combined organic layers were washed with water (2 × 300 mL), sat. aq. $NaHCO_3$ (2 × 300 mL) and sat. aq. NaCl (2 × 300 mL), dried over anhyd. Na_2SO_4 and evaporated to give a yellow oil. The oil was placed under vacuum overnight which caused it to solidify. Recrystallization from ethanol (saturated with water at the boiling point) gave 8.6 g of slightly tan formyl pyrrole in 82% yield. It had mp 84-86°C (Lit.[29] 87°C); IR (KBr) ν: 3420, 3080, 2900, 1730, 1700, 1645 cm^{-1}; ^{1}H-NMR ($CDCl_3$) δ: 1.24 (t, 2H, J=7.3 Hz), 1.38 (t, 2H, J=7.3 Hz), 2.34 (s, 3H), 2.54 (t, 3H, J=7.3 Hz), 3.04 (t, 3H, J=7.3 Hz), 4.12 (q, 2H, J=7.3 Hz), 4.36 (q, 2H, J=7.3 Hz), 9.48 (brs, 1H, NH), 9.78 (s, 1H, CHO) ppm; and ^{13} C-NMR ($CDCl_3$) δ: 8.20 (q), 14.03 (q), 14.07 (q), 19.69 (t), 34.54 (t), 60.18 (t), 60.92 (t), 124.36 (s), 129.63 (s), 129.64 (s), 130.02 (s), 161.83 (s), 172.67 (s), 179.10 (s) ppm.

2,3,7-Trimethyl-(10*H*)-dipyrrin-1-one-8-propanoic acid (12) (3-nor-neo-xanthobilirubic acid). 3,4-Dimethyl-3-pyrrolin-2-one[17a] (3.0 g, 27 mmol) and (**10**) (6.5 g, 23 mmol) were placed in a 500 mL flask containing a magnetic stir bar. To the mixture of solids was added 250 mL of 95% ethanol and 60 mL of 4M aq. KOH, and the solution was allowed to reflux overnight. The cooled solution was extracted with ether to remove any unsaponified compounds, and the aqueous layer was acidified to pH 3 with concentrated HCl. A bright yellow solid dipyrrinone (**11**) separated and was repeatedly washed with water and collected by centrifugation. After drying, this afforded 6.3 g (84%) of the desired dipyrrinone diacid (**11**). It had mp 220°C (dec.); ^{1}H-NMR ($(CD_3)_2SO$) δ: 1.75 (s, 3H), 2.01 (s, 3H), 2.03 (s, 3H), 2.33 (t, 2H, J=7.5 Hz), 2.85 (t, 2H, J=7.5 Hz), 5.88 (s, 1H), 10.39 (brs, 1H, NH), 10.98 (s, 1H, NH) 12.02 (brs, 2H, CO_2H) ppm; and ^{13} C-NMR ($(CD_3)_2SO$) δ: 8.16 (q), 8.80 (q), 9.37 (q), 20.09 (t), 34.63 (t), 95.93 (d), 121.48 (s), 122.07 (s), 126.21 (s), 127.24 (s), 129.04 (s), 134.21 (s), 141.69 (s), 161.80 (s), 172.51 (s), 173.81 (s) ppm. The product (**11**) was decarboxylated directly in the next step without further purification.

Diacid (**11**) (5.39 g,19.7mmol), KOAc trihydrate (24.3g) and NaOAc trihydrate (22.6 g) were placed in a mortar and ground to make an intimate mixture. The yellow paste was carefully transferred to a 250 mL round bottom flask containing a magnetic stir bar, and slowly lowered into an oil bath at 120°C. The mixture melted and the material clinging to the sides of the flask was washed down by basting the outer walls of the flask with hot oil using a Pasteur pipette. The temperature was increased to 130°C and decarboxylation commenced as evidenced by profuse bubbling from the molten mixture. The temperature was allowed to remain at 130-150°C for 20 min., and then the flask was allowed to cool. The resultant solid residue was dissolved in water and acidified to pH 3 with concentrated HCl which caused precipitation of an olive green solid. This solid was repeatedly washed with water and collected by centrifugation. Drying overnight in a vacuum desiccator over P_2O_5 yielded 4.06 g (87.5%) of the desired dipyrrinone (**12**). It had mp 245-248°C (lit.[17a] mp 245-247°C); IR (KBr) ν: 3345, 3125, 2910, 1615 cm^{-1}; UV-Vis (CH_3OH): ε (λ^{max}) = 27000 (395); (DMSO): ε (λ^{max}) = 30000 (395); ^{1} H-NMR ($CDCl_3$) δ: 1.96 (s, 3H), 2.21 (s, 3H), 2.23 (s, 3H), 2.70 (t, 2H, J=7.2 Hz), 2.80 (t, 2H, J=7.2 Hz), 6.65 (s, 1H), 7.02 (s, 1H), 9.54 (brs, 1H, NH), 11.98 (brs, 1H, NH) ppm; and ^{13} C-NMR ($CDCl_3$) δ: 7.82 (q), 9.56 (q), 10.11 (q), 20.13 (t), 34.44 (t), 109.54 (d), 121.40 (s), 123.81 (s), 124.25 (s), 125.36 (s), 127.83 (s), 129.45 (s), 145.82 (s), 172.22 (s), 179.98 (s) ppm.

10-Isopropyl-8,12-bis-(2-carboxyethyl)-2,3,7,13,17,18-hexamethyl-1,10,19,21,23,24-hexahydro-1,19-dioxobilin (1). 3-Nor-neo-xanthobilirubic acid (**12**)[17a] (548 mg, 2.00 mmol.) was placed in a 25 mL round bottom flask along with a small magnetic stir bar. The flask was then fitted with a rubber septum, and 6 mL of dichloromethane was added. After flushing the system with N_2 for several minutes, isobutyraldehyde (99.9 μL, 1.10 mmol) and TFA (500 μL) were added using a syringe. Upon addition of the TFA, the mixture became homogeneous and reddish orange. It was allowed to stir under N_2 at room temperature for 8 hrs; the dark solution was then taken up in 100 mL of dichloromethane, and washed with water and saturated aq. NaCl. After drying over anhyd. Na_2SO_4, the solvent was evaporated to give a dark solid. This solid was initially purified by flash-column chromatography on silica gel, eluting with dichloromethane-methanol 100:2 (by vol). The solvents were removed under vacuum to give an orange solid. Further purification was carried out by radial chromatography eluting with dichloromethane-methanol 100:2 (by vol.) to afford 464 mg (77%) of the desired bright yellow pigment. It had mp 260°C (dec); IR (KBr) ν: 3410, 3258, 2954, 2916, 2364, 1687, 1654, 1616, 1437, 1404, 1363, 1260, 1186, 1008, 939, 843 cm^{-1}; and ^{1}H-NMR and ^{13}C-NMR reported in Tables 1 and 2.

Anal. Calcd. for $C_{34}H_{42}N_4O_6$ (602.7): C, 67.75; H, 7.02; N, 9.30.
Calcd. for $C_{34}H_{42}N_4O_6 \cdot CH_3OH$ (636.7): C, 64.83; H, 7.56; N, 8.41.
Found: C, 64.84; H, 7.13; N, 8.63.

10-Isopropyl-8,12-bis-(2-methoxycarbonylethyl)-2,3,7,13,17,18-hexamethyl-1,10,19,21,23,24-hexahydro-1,19-dioxobilin (7). Cesium carbonate (130 mg, 0.674 mmol) followed by iodomethane (25.2 μL, 0.405 mmol) was added to a solution of (**1**) (100 mg, 0.165 mmol) in dry DMF (3.50 mL) and stirred at room temperature overnight. The yellow solution was then taken up in 50 mL of dichloromethane and extracted with water (3 × 100 mL), dried over anhydr. Na_2SO_4, and evaporated to give an oil still containing some DMF. The oil was placed under high vacuum for a day, and the solid residue was purified by radial chromatography. Elution with dichloromethane-methanol 100:3 (by vol) afforded 88.7 mg of the desired diester (**7**) as a bright yellow solid (85%). It had mp 250°C (dec). IR (KBr) ν: 3399, 2953, 2867, 2363, 1737, 1676, 1652, 1628, 1437, 1384, 1364, 1268, 1244, 1168, 1054, 944, 901, 846, 754, 723, 692, 580 cm^{-1}; and ^{1}H-NMR ($CDCl_3$) δ: 0.64 (d, 6H, 6.40 Hz), 1.39 (brs, 6H), 1.93 (s, 6H), 2.11 (s, 6H), 2.47 (t, 4H, J=7.80 Hz), 2.72 (m, 1H), 2.85 (t, 4H, J=7.80 Hz), 3.74 (s, 6H), 3.74 (d, 1H, J=11.30 Hz), 5.85 (s, 2H), 9.92 (brs, 4H, NH) ppm. ^{1}H-NMR (($CD_3)_2SO$) δ: 0.84 (d, 6H, 6.40 Hz), 1.74 (s, 6H), 1.92 (s, 6H), 2.02 (s, 6H), 2.46 (t, 4H, J=7.80 Hz), 2.65 (t, 4H, J=7.80 Hz), 2.70 (m, 1H), 3.38 (s, 6H), 3.75 (d, 1H, J=11.75 Hz), 5.87 (s, 2H), 9.83 (brs, 2H, NH), 9.93 (brs, 2H, NH) ppm. ^{13}C-NMR data are reported in Table 1. An analytical sample was prepared by the addition of hexane to a dichloromethane solution of the pigment followed by slow evaporation of the solvents under a stream of nitrogen. The resultant bright yellow crystals were collected by filtration and dried over P_2O_5 in a drying pistol overnight.

Anal. Calcd. for $C_{36}H_{46}N_4O_6$ (630.8): C, 68.55; H, 7.35; N, 8.89.
Found: C, 68.13; H, 7.41; N, 8.64.

10-Isopropyl-2,3,7,8,12,13,17,18-octamethyl-1,10,19,21,23,24-hexahydro-1,19-dioxobilin (5). 2,3,7,8-Tetramethyl-(10 *H*)-dipyrrin-1-one (**13**)[19] (432 mg, 2.00 mmol) was converted to (**5**) exactly as described for the synthesis of (**1**). The crude coupled rubin was initially purified by flash-column chromatography on silica gel eluting with dichloromethane-methanol 100:1 (by vol) to give an orange solid. Further purification was carried out by radial chromatography, eluting with dichloromethane-methanol 100:1 (by vol) to afford 252.7 mg (52%) of the desired yellow-orange pigment. It had mp 260°C (dec); IR (KBr) ν: 2966, 2919, 1678, 1648, 1631, 1437,

1378, 1237, 1166, 937, 749, 726, 685 cm^{-1}; and ^{1}H-NMR ($CDCl_3$) δ: 0.67 (d, 6H, J=5.85 Hz), 1.42 (s, 6H), 1.92 (s, 6H), 2.05 (s, 6H), 2.07 (s, 6H), 2.74 (m, 1H), 3.81 (d, 1H, J=11.23 Hz), 5.92 (s, 2H), 9.98 (brs, 2H, NH), 11.00 (brs, 2H, NH) ppm. ^{13}C-NMR data are reported in Table 1. An analytical sample was prepared by the addition of methanol to a dichloromethane solution of the pigment followed by slow evaporation of the solvents under a stream of nitrogen. The resultant yellow-orange crystals were filtered and dried over P_2O_5 in a drying pistol overnight.

Anal. Calcd. for $C_{30}H_{38}N_4O_2$ (486.7): C, 74.03; H, 7. 88; N, 11.52.
Calcd. for $C_{30}H_{38}N_4O_2 \cdot ½\ CH_3OH$ (502.7): C, 72.88; H, 8.24; N, 11.15.
Found: C, 72.84; H, 7.91; N, 11.00.

10-Isopropylidene-8,12-bis-(2-methoxycarbonylethyl)-2,3,7,13,17,18-hexamethyl-1,19,21,24-tetrahydro-1,19-dioxobilin (8). To a solution of 0.100 mmol isopropyl rubin dimethyl ester (**7**) (63.0 mg) in 30 mL of dry THF was added an equivalent amount (0.100 mmol, 22.7 mg) of DDQ in 10 mL of dry THF and the mixture was stirred at room temperature for 30 min. Upon addition of the DDQ solution the rubin solution underwent a series of gradual color changes. The brownish-yellow mixture was then poured into a two-phase system consisting of 100 mL of $CHCl_3$ and 100 mL of 2% aqueous ascorbic acid, and extracted with $CHCl_3$. (For better separation, sat. NaCl solution may be added.) The combined organic layers were washed with sat. aq. Na_2CO_3 (2 × 100 mL), then with sat. aq. NaCl (2 × 100 mL), and finally dried over anhydrous Na_2SO_4. The brownish-yellow solution was then evaporated to give a brown solid. The crude product was purified by radial chromatography eluting with 100:3 (by vol) dichloromethane-methanol) to give 27.1 mg (43%) of the desired yellow pigment (**8**). Repeated chromatography is necessary as starting material and product have very similar R_f's. It had mp 270°C (dec.); IR (KBr) ν: 3349, 2921, 2363, 1735, 1663, 1636, 1508, 1438, 1364, 1262, 1170, 943, 758, 692 cm^{-1}; and ^{1}H-NMR ($CDCl_3$) δ: 1.61 (brs, 6H, 1.73 (s, 6H), 1.98 (s, 6H), 2.12 (s, 6H), 2.49 (t, 4H, J=7.80 Hz), 2.72 (t, 4H, J=7.80 Hz), 3.69 (s, 6H), 5.94 (s, 2H), 9.95 (brs, 4H, NH) ppm. ^{1}H-NMR ($(CD_3)_2SO$) δ: 1.75 (s, 6H), 1.80 (s, 6H), 1.97 (s, 6H), 2.04 (s, 6H), 2.22 (t, 4H, J=7.80 Hz), 2.35 (t, 4H, J=7.80 Hz), 3.33 (s, 6H), 5.90 (s, 2H), 9.99 (brs, 2H, NH), 10.37 (brs, 2H, NH) ppm. ^{13}C-NMR data are reported in Table 1.

Anal. Calcd. for $C_{36}H_{44}N_4O_6$ (628.7): C, 68.77; H, 7.05; N, 8.91.
Calcd. for $C_{36}H_{44}N_4O_6 \cdot H_2O$ (646.6): C, 66.85; H, 7.17; N, 8.66.
Found: C, 67.10; H, 6.80; N, 8.35.

10-Isopropylidene-8,12-bis-(2-carboxyethyl)-2,3,7,13,17,18-hexamethyl-1,19,21,24-tetrahydro-1,19-dioxobilin (2). To a 50 mL RB flask was added 22.0 mg (0.035 mmol) isopropylrubin ester (**8**) and 10.0 mg (0.057 mmol) of ascorbic acid. The solids were dissolved in 14 mL of THF-MeOH 1:1 (by vol.) and then 14 mL of 0.1 M NaOH was added. The orange solution was stirred at 37-40°C for 90 min. The cooled basic solution was extracted with chloroform, and the aqueous layer was acidified with glacial acetic acid, then extracted with chloroform. The organic layer was washed with water, dried over anhydr. Na_2SO_4 and evaporated to give a yellow residue which was purified by radial chromatography. Elution with 100:2 (by vol) dichloromethane-methanol afforded 16.1 mg (76%) of the desired diacid (**2**). It had mp 310°C (dec.); IR (KBr) ν: 3414, 2921, 1694, 1649, 1620, 1438, 1406, 1402, 1361, 1259, 1179, 939, 838, 755, 692 cm^{-1}; and ^{1}H-NMR and ^{13}C-NMR reported in Tables 1 and 2.

Anal. Calcd. for $C_{34}H_{40}N_4O_6$ (600.7): C, 67.98; H, 6.71; N, 9.33.
Found: C, 67.65; H, 6.76; N, 9.08.

10-Isopropylidene-2,3,7,8,12,13,17,18-octamethyl-1,19,21,24-tetrahydro-1,19-dioxobilin (6). Permethyl isopropylrubin (**5**) (48.6 mg, 0.100 mmol) was converted to (**6**) exactly as described for the synthesis of (**8**). The crude product was purified by radial chromatography eluting with 100:2 (by vol) dichloromethane-methanol) to give 47.2 mg (98.0 %) of the desired yellow pigment (**6**). It had mp 285 °C (dec.); IR (KBr) ν: 2912, 2353, 1680, 1664, 1647, 1636, 1508, 1446, 1382, 1253, 1166, 1096, 938, 816 cm^{-1}; and ^{1}H-NMR ($CDCl_3$) δ: 1.57 (s, 6H), 1.72 (s, 6H), 1.94 (s, 6H), 1.95 (s, 6H), 2.08 (s, 6H), 5.97 (s, 2H), 10.33 (brs, 4H, NH) ppm; ^{1}H-NMR ($(CD_3)_2SO$) δ: 1.54 (s, 6H), 1.71 (s, 6H), 1.77 (s, 6H), 1.96 (s, 6H), 1.98 (s, 6H), 5.85 (s, 2H), 9.98 (brs, 2H, NH), 10.02 (brs, 2H, NH) ppm; ^{13}C-NMR data are reported in Table 1.

Anal. Calcd. for $C_{30}H_{36}N_4O_2$ (484.6): C, 74.35; H, 7.49; N, 11.56.
Found: C, 74.41; H, 7.81; N, 11.62.

Acknowledegments: We thank the National Institutes of Health (HD 17779) for generous support and the National Science Foundation (CHE-9214294) for assistance in purchasing the 500 MHz NMR spectrometer used in this work. Special thanks go to Mr. Lew Cary for his assistance in the NMR experiments. Ari Kar is a Wilson Graduate Fellowship Awardee.

REFERENCES

1. McDonagh, A.F. *Bile Pigments: Bilatrienes and 5,15-Biladienes.* In *The Porphyrins*; Dolphin, D., Ed.; Academic Press: New York, **1979**, *6*, 293.
2. Schmid, R.; McDonagh, A.F. Hyperbilirubinemia. In *The Metabolic Basis for Inherited Diseases* (Stanbury, J.B.; Wyngaarden, J.B.; Frederickson, D.S., Eds.), McGraw-Hill: NY, **1978**, pp. 1221-57.
3. Chowdury, J.R., Wolkoff, A.W., Chowdury, N.R., and Arias, I.M. "Hereditary Jaundice and Disorders of Bilirubin Metabolism" in *The Metabolic and Molecular Bases of Inherited Disease* (Scriver, C.R., Beaudet, A.L., Sly, W.S., and Valle, D., eds.) McGraw-Hill, Inc., New York, *Vol. II*, **1995**, chap. 67, 2161-2208.
4. (a) Thomas, S.R.; Neuzil, J.; Mohr, D.; Stocker, R. *Amer. J. Clin. Nutrition*, **1995**, *62*, 13575-13645.
   (b) Dennery, P.A.; McDonagh, A.F.; Spitz, D.R.; Rodgers, P.A.; Stevenson, D.K. *Free Radical Biol. Med.* **1995**, *19*, 395-404.
5. Berk, P.D.; Noyer, C. *Seminars Liver Dis.*, **1994**, *14*, 323-394.
6. (a) Bonnett, R.; Davies, J. E.; Hursthouse, M. B.; Sheldrick, G. M. *Proc. R. Soc. London, Ser. B*, **1978**, *202*, 249-268.
   (b) LeBas, G.; Allegret, A.; Mauguen, Y.; DeRango, C.; Bailly, M. *Acta Crystallogr., Sect. B*, **1980**, *B36*, 3007-3011.
7. Person, R.V.; Peterson, B.R.; Lightner, D.A. *J. Am. Chem. Soc.*, **1994**, *116*, 42-59.
8. Mugnoli, A.; Manitto, P.; Monti, D. *Acta Crystallogr., Sect. C*, **1983**, *39*, 1287-1291.
9. (a) Shelver, W.H.; Rosenberg, H.; Shelver, W.H. *Intl. J. Quantum Chem.*, **1992**, *44*, 141-163.
   (b) Shelver, W.L.; Rosenberg, H.; Shelver, W.H. *J. Molec. Struct.*, **1994**, *312*, 1-9.
10. Kaplan, D.; Navon, G. *Israel J. Chem.* **1983**, *23*, 177-186.

11. Trull, F.R.; Ma, J.S.; Landen, G.L.; Lightner, D.A. *Israel J. Chem.* **1983**, *23*, 211-218.
12. (a) Falk, H.; Müller, N. *Monatsh. Chem.* **1982**, *112*, 1325-1332.
    (b) Falk, H.; Müller, N. *Tetrahedron* **1983**, *39*, 1875-1885.
13. Falk, H. *The Chemistry of Linear Oligopyrroles and Bile Pigments*; Springer Verlag: New York/Wien, 1989.
14. (a) Dörner, T.; Knipp, B.; Lightner, D.A. *Tetrahedron* **1997**, *53*, 2697-2716.
    (b) Nogales, D.; Lightner, D.A. *J. Biol. Chem.* **1995**, *270*, 73-77.
15. Trull, F.R.; Shrout, D.P.; Lightner, D.A. *Tetrahedron* **1992**, *48*, 8189-8198.
16. Boiadjiev, S.E.; Person, R.V.; Puzicha, G.; Knobler, C.; Maverick, E.; Trueblood, K.N.; Lightner, D.A. *J. Am. Chem. Soc.* **1992**, *114*, 10123-10133.
17. (a) Xie, M.; Lightner, D.A. *Tetrahedron* **1993** *49*, 2185-2200.
    (b) Xie, M.; Holmes, D.L.; Lightner, D.A. *Tetrahedron* **1993**, *49*, 9235-9250.
18. Falk, H.; Müller, N.; Wöss, H. *Monatsh. Chem.*, **1989**, *120*, 35-43.
19. Montforts, F.P.; Schwartz, U.M. *Liebigs Ann. Chem.* **1985**, 1228-1253.
20. Thyrann, T.; Lightner, D.A. *Tetrahedron Lett.* **1995**, *36*, 4345-4348.
21. Trull, F.R.; Franklin, R.W.; Lightner, D.A. *J. Heterocyclic Chem.* **1987**, *24*, 1573-1579.
22. Nogales, D.F.; Ma, J-S.; Lightner, D.A. *Tetrahedron* **1993**, *49*, 2361-2372.
23. (a) Boiadjiev, S.E.; Anstine, D.T.; Lightner, D.A. *J. Am. Chem. Soc.* **1995**, *117*, 8727-8736.
    (b) Boiadjiev, S.E.; Anstine, D.T.; Maverick, E.; Lightner, D.A. *Tetrahedron: Asymm.* **1995**, *6*, 2253-2270.
24. Boiadjiev, S.E.; Lightner, D.A. *Tetrahedron: Asymmetry* **1997**, *8*, 2115-2129.
25. Molecular mechanics calculations and molecular modelling was carried out on an Evans and Sutherland ESV-10 workstation using version 6.0 of SYBYL (Tripos Assoc., St. Louis, MO). [See R.V. Person, B.R. Peterson and D.A. Lightner, *J. Am. Chem. Soc.*, **116**, 42 (1994).] The ball and stick drawings were created from the atomic coordinates of the molecular dynamics structures using Müller and Falk's "Ball and Stick" program (Cherwell Scientific, Oxford, U.K.) for the Macintosh.
26. Boiadjiev, S.E.; Pfeiffer, W.P.; Lightner, D.A. *Tetrahedron* **1997**, *53*, 14547-14564.
27. Lightner, D.A.; Gawroński, J.K.; Wijekoon, W.M.D. *J. Am. Chem. Soc.* **1987**, *109*, 6354-6362.
28. Kasha, M.; El-Bayoumi, M.A.; Rhodes, W. *J. Chim. Phys.-Chim. Biol.* **1961**, *56*, 916-925.
29. (a) Battersby, A.R.; Hodgson, G.L.; Ihara, M.; McDonald, E.; Saunders, J. *J. Chem. Soc. Perkin 1*, **1973**, *23*, 2923-2935.
    (b) Inhoffen, H.H.; Fattinger, F.; Schwarz, N. *Liebigs. Ann. Chem.* **1974**, *3*, 412-438.